The Plant Cell, Vol. 29: 1024–1038, May 2017, www.plantcell.org © 2017 ASPB.

ELF18-INDUCED LONG-NONCODING RNA Associates with Mediator to Enhance Expression of Innate Immune Response Genes in Arabidopsis

Jun Sung Seo,[a,b,1] Hai-Xi Sun,[a,1,2] Bong Soo Park,[a,b] Chung-Hao Huang,[a,c] Shyi-Dong Yeh,[c] Choonkyun Jung,[a,3,4] and Nam-Hai Chua[a,b,4]

[a] Laboratory of Plant Molecular Biology, Rockefeller University, New York, New York 10065
[b] Temasek Life Sciences Laboratory, National University of Singapore, 117604, Singapore
[c] Department of Plant Pathology, National Chung Hsing University, Taichung 40227, Taiwan

ORCID ID: 0000-0002-8991-0355 (N.-H.C.)

The plant immune response is a complex process involving transcriptional and posttranscriptional regulation of gene expression. Responses to plant immunity are initiated upon the perception of pathogen-associated molecular patterns, including peptide fragment of bacterial flagellin (flg22) or translation elongation factor Tu (elf18). Here, we identify an *Arabidopsis thaliana* long-noncoding RNA, designated ELF18-INDUCED LONG-NONCODING RNA1 (ELENA1), as a factor enhancing resistance against *Pseudomonas syringe* pv *tomato* DC3000. ELENA1 knockdown plants show decreased expression of *PATHOGENESIS-RELATED GENE1* (*PR1*) and the plants are susceptible to pathogens. By contrast, plants overexpressing ELENA1 show elevated *PR1* expression after elf18 treatment and display a pathogen resistance phenotype. RNA-sequencing analysis of ELENA1-overexpressing plants after elf18 treatment confirms increased expression of defense-related genes compared with the wild type. ELENA1 directly interacts with Mediator subunit 19a (MED19a) and affects enrichment of MED19a on the *PR1* promoter. These results show that MED19a regulates *PR1* expression through ELENA1. Our findings uncover an additional layer of complexity, implicating long-noncoding RNAs in the transcriptional regulation of plant innate immunity.

INTRODUCTION

Plants and animals are confronted with constant risk of infections by various microorganisms in their natural habitats. Like animals, plants have evolved a repertoire of pattern recognition receptors (PRRs) that recognize molecular signatures typical of entire classes of microbial pathogens. Pathogen-associated molecular patterns (PAMPs) include bacterial flagellin, translation elongation factor Tu (EF-Tu), peptidoglycans, lipopolysaccharides, and fungal cell wall-derived chitin fragments (Jones and Dangl, 2006; Boller and Felix, 2009). Perception of different PAMPs by cognate PRRs triggers innate immune responses that restrict pathogen propagation, and this series of signaling events is designated PAMP-triggered immunity (PTI) (Jones and Dangl, 2006). The best-characterized bacterial PAMPs recognized by plants are flg22 and elf18, which are derived from flagellin and EF-Tu, respectively (Kunze et al., 2004). flg22 and elf18 are recognized by FLAGELLIN SENSING2 (FLS2) and EF-Tu RECEPTOR (EFR), respectively, and these receptors belong to the leucine-rich repeat-receptor kinase family XII in *Arabidopsis thaliana* (Zipfel et al., 2006).

Following pathogen detection by PRRs, plants are able to mount a number of defense responses, including production and secretion of antimicrobial compounds and defense-related proteins (van Loon et al., 2006; Bednarek, 2012). Pathogenesis-related (PR) proteins are an important class of inducible defense-related proteins in various plant species, and they function as key players in an immune surveillance mechanism that protects plants primarily against invasion by microorganisms (van Loon et al., 2006). *PR1* expression is highly responsive to salicylic acid (SA) and bacterial pathogens, and its transcriptional regulation has been extensively studied (Pajerowska-Mukhtar et al., 2013). As a key factor in *PR1* expression, NONEXPRESSER OF PR GENES1 orchestrates *PR1* transcriptional activity in concert with the TGA family of basic region/leucine zipper motif transcription factors (TFs) (Kesarwani et al., 2007; Gatz, 2013) and WRKY TF family (Yu et al., 2001; Eulgem and Somssich, 2007)

TFs typically have effector (activator or repressor) domains that are separated from their DNA binding domains, and they interact with transcriptional regulators. The Mediator complex is a general target of TF effector domains; moreover, as different TFs bind to different Mediator subunits, multiple TFs might bind to the Mediator complex at the same time (Allen and Taatjes, 2015). A basic function of Mediator is to communicate regulatory signals from TFs directly to the RNA polymerase II (Pol II) enzyme. The precise mechanisms by which the Mediator complex regulates Pol II

[1] These authors contributed equally to this work.
[2] Current address: Wilmar Innovation Centre, 1 Research Link, National University of Singapore, 117604, Singapore.
[3] Current address: Graduate School of International Agricultural Technology and Crop Biotechnology Institute/GreenBio Science and Technology, Seoul National University, Pyeongchang 25354, Korea.
[4] Address correspondence to jasmin@snu.ac.kr or chua@mail.rockefeller.edu.
The author responsible for distribution of materials integral to the findings presented in this article in accordance with the policy described in the Instructions for Authors (www.plantcell.org) is: Nam-Hai Chua (e-mail chua@mail.rockefeller.edu).
www.plantcell.org/cgi/doi/10.1105/tpc.16.00886

activity remain poorly understood, but they clearly involve extensive protein-protein interactions between Mediator, Pol II, and other general and gene-specific TFs. Through those interactions, the Mediator complex is involved in a broad range of transcriptional events, including transcription initiation, transcript elongation, changes in chromatin architecture, and enhancer-promoter gene looping (Allen and Taatjes, 2015). In plants, quite a number of Mediator subunits have been characterized as important regulators for different signaling networks in response to various developmental as well as environmental changes. So far, at least nine Mediator subunits, MED8, 14, 15, 16, 18, 19, 21, 25, and CDK8, have been implicated in defense signaling (Samanta and Thakur, 2015).

High-resolution RNA sequencing (RNA-seq) analyses in animals and plants have revealed that the transcriptional landscape in eukaryotes is much more complex than previously envisioned and pervasive transcription seems to be a widespread feature of all eukaryotic genomes (Chekanova et al., 2007; Kapranov et al., 2007; Guttman et al., 2009; Liu et al., 2015). Early studies questioned the biological relevance of long-noncoding RNAs (lncRNAs; longer than 200 nucleotides) because of their low expression levels and lack of sequence conservation. But recently, a variety of types and origins of lncRNAs has been identified and shown to play important roles in transcriptional regulation and chromatin modification (Rinn and Chang, 2012; Kung et al., 2013; St Laurent et al., 2015). In plants, the regulatory roles of lncRNAs are only beginning to be recognized, and the molecular basis of lncRNA-mediated gene regulation is still poorly understood. So far, plant lncRNAs have been shown to play key roles in phosphate signaling, flowering time, auxin transport, root organogenesis, and seedling photomorphogenesis (Franco-Zorrilla et al., 2007; Swiezewski et al., 2009; Heo and Sung, 2011; Ariel et al., 2014; Bardou et al., 2014; Wang et al., 2014).

Previously, we performed a custom lncRNA array analysis with elf18-treated Arabidopsis seedlings to screen for PAMP-responsive lncRNAs (Liu et al., 2012). We selected multiple lncRNA candidates that were highly induced by elf18 treatment, designated as ELENAs (ELF18-INDUCED LONG-NONCODING RNAs) for further analysis. Among them, we found that ELENA1 acts as a positive regulator of resistance against bacterial pathogens by analyzing ELENA1 knockdown (KD) and overexpressing (OX) plants. Genome-wide transcriptome analysis of ELENA1 OX plants showed elevated expression of defense-related genes, including *PR1*. Transcriptional regulation of *PR1* by ELENA1 was brought about by interaction with MED19a and its enrichment on the *PR1* promoter. Taken together, our results provide evidence that the lncRNA ELENA1 plays a positive role in plant innate immunity by regulating *PR1* expression.

RESULTS

ELENA1 Expression Is Induced by elf18 and flg22 in an EFR- and FLS2-Dependent Manner

We screened for polyadenylated lncRNAs in response to elf18 treatment (Liu et al., 2012). Among them, *ELENA1* (At4g16355) is located between *CALCINEURIN B-LIKE6* (At4g16350) and another locus (At4g16360), encoding a putative protein kinase (Figure 1A). The ELENA1 transcript level was induced by both elf18 and flg22 treatments and reached a maximum at 12 h after treatment, but it was not responsive to SA treatment (Figure 1B).

To define the promoter regions responsible for ELENA1 expression responding to elf18 and flg22, two 5′ upstream fragments of *ELENA1*, 1.5 kb (P_{1500}) and 0.2 kb (P_{200}), were fused to the *GUS* coding sequence and transformed into Arabidopsis (Figure 1C). Histochemical GUS staining of transgenic plants showed that elf18- and flg22-responsive GUS activity was detected only in leaves of the P_{1500}*:GUS* lines, but not in the P_{200}*:GUS* lines (Figure 1D). These results indicate that the *ELENA1* promoter responds to elf18 and flg22 and the region between 0.2 and 1.5 kb upstream of the *ELENA1* promoter contains putative *cis*-acting elements required for elf18 and flg22 responsiveness.

In Arabidopsis, EFR (At5g20480) and FLS2 (At5g46330) function as receptors of elf18 and flg22, respectively (Gómez-Gómez and Boller, 2000; Zipfel et al., 2006). To investigate whether ELENA1 transcription was regulated by receptor-dependent pathways, we examined ELENA1 transcript levels in each receptor knockout (KO) mutant, *efr-2* and *fls2*. Transcript induction after elf18 treatment was abolished in *efr-2* mutants (Figure 1E), and it was also blocked in *fls-2* after flg22 treatment (Figure 1F). These results provide evidence that ELENA1 transcription is regulated through PRR-dependent pathways.

ELENA1 KD and OX Plants Show Altered Responses to *Pst* DC3000 and Changes in *PR1* Expression

To investigate the function of ELENA1 in plant innate immunity, we generated ELENA1 KD transgenic plants using an artificial miRNA (Niu et al., 2006) (Supplemental Figure 1A) and selected two independent lines (KD-10 and KD-20) showing significantly reduced ELENA1 transcript levels (Supplemental Figure 1B). We also generated ELENA1 OX transgenic plants using a 35S promoter (Supplemental Figure 2A) and selected two independent lines (OX-16 and OX-29) showing high expression of ELENA1 (Supplemental Figure 2B). Selected KD lines and OX lines were inoculated with *Pseudomonas syringae* pv *tomato* DC3000 (*Pst* DC3000) to investigate defense phenotypes. Leaf chlorosis and bacterial growth assay showed that KD lines were more susceptible to *Pst* DC3000, whereas OX lines were more resistant (Figures 2A and 2B). In addition, *PR1* (*At2g14610*) expression after *Pst* DC3000 infection was enhanced in OX lines but reduced in KD lines compared with the wild type (Col-0) (Figure 2C). These results indicate that ELENA1 is a positive regulator of resistance against *Pst* DC3000.

We also examined the expression of *PR1* and *PR2* (*At3g57260*) in transgenic plants with altered ELENA1 expression after elf18 treatment. *PR1* and *PR2* expression were reduced in KD lines, but enhanced in OX lines compared with the wild type (Figures 2D and 2E). Overall, our results show that ELENA1 is a positive regulator in *PR* gene expression and resistance against bacterial pathogen.

ELENA1 Functions as a Bona Fide lncRNA

It has been recently reported that several lncRNAs could encode small peptides and function as peptide-coding genes (Anderson

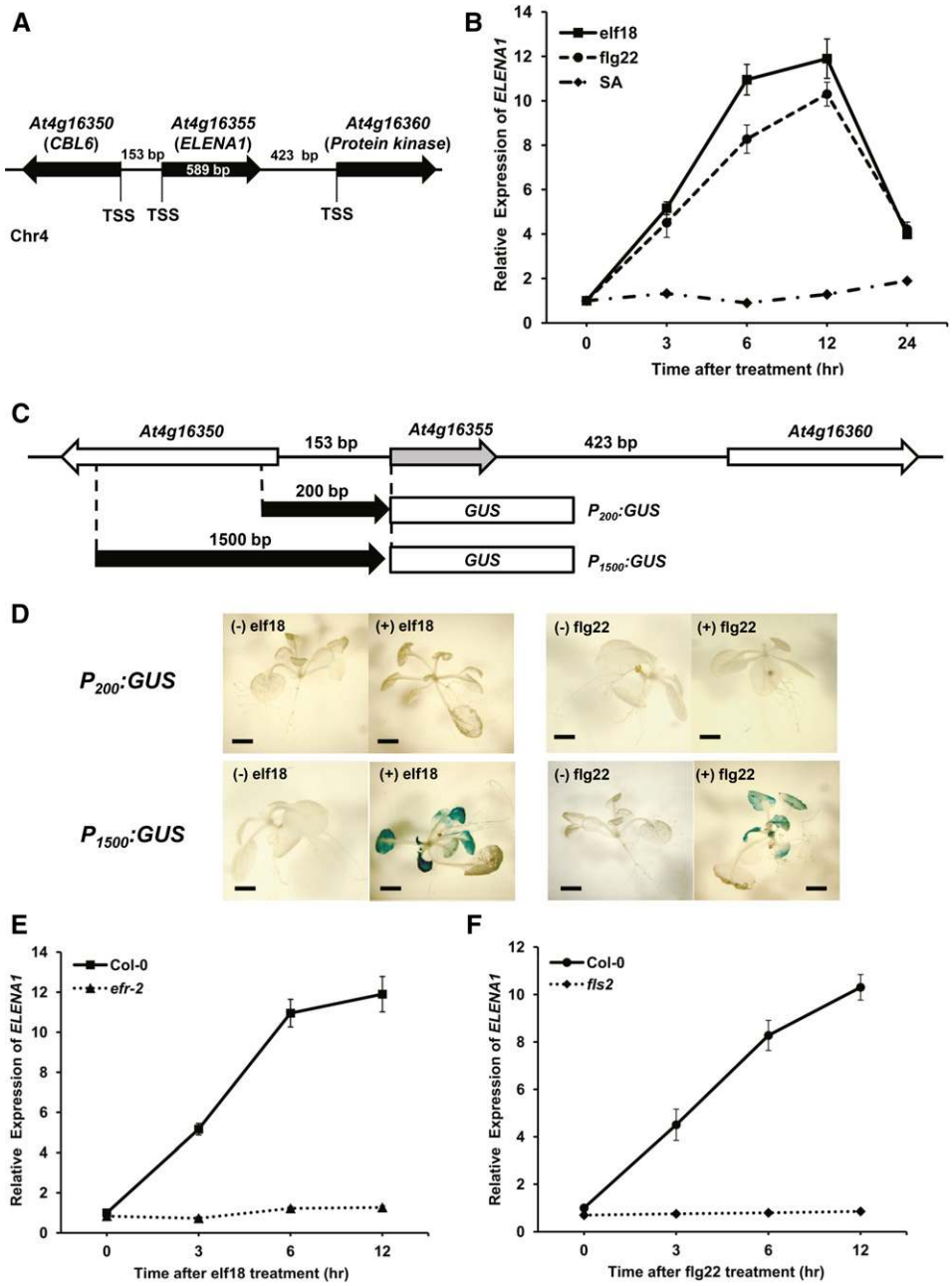

Figure 1. ELENA1 Transcript Levels Are Induced by elf18 and flg22.

(A) Schematic representation of the *ELENA1* genomic location. TSS, transcription start site.
(B) Time-course analysis of ELENA1 expression levels after treatment. Ten-day-old wild-type (Col-0) seedlings were treated with 5 μM elf18, 5 μM flg22, or 1 mM SA.
(C) Schematic representation of P_{ELENA1}:*GUS* constructs. P_{200} is 200 bp upstream of the transcription start site, and P_{1500} is 1500 bp upstream.
(D) Histochemical staining of P_{200}:*GUS* and P_{1500}:*GUS* transgenic plants with (+) or without (−) elf18 or flg22 treatment for 6 h. Bars = 2 mm.
(E) Time-course analysis of ELENA1 transcript levels in *efr-2* mutant after elf18 treatment.
(F) Time-course analysis of ELENA1 transcript levels in *fls2* mutant after flg22 treatment. Ten-day-old seedlings were treated with 5 μM elf18 or 5 μM flg22.
For **(B)**, **(E)**, and **(F)**, transcript levels were normalized to *ACT2* expression levels. Bars represent average ± SD (n = 3 independent seedling pools).

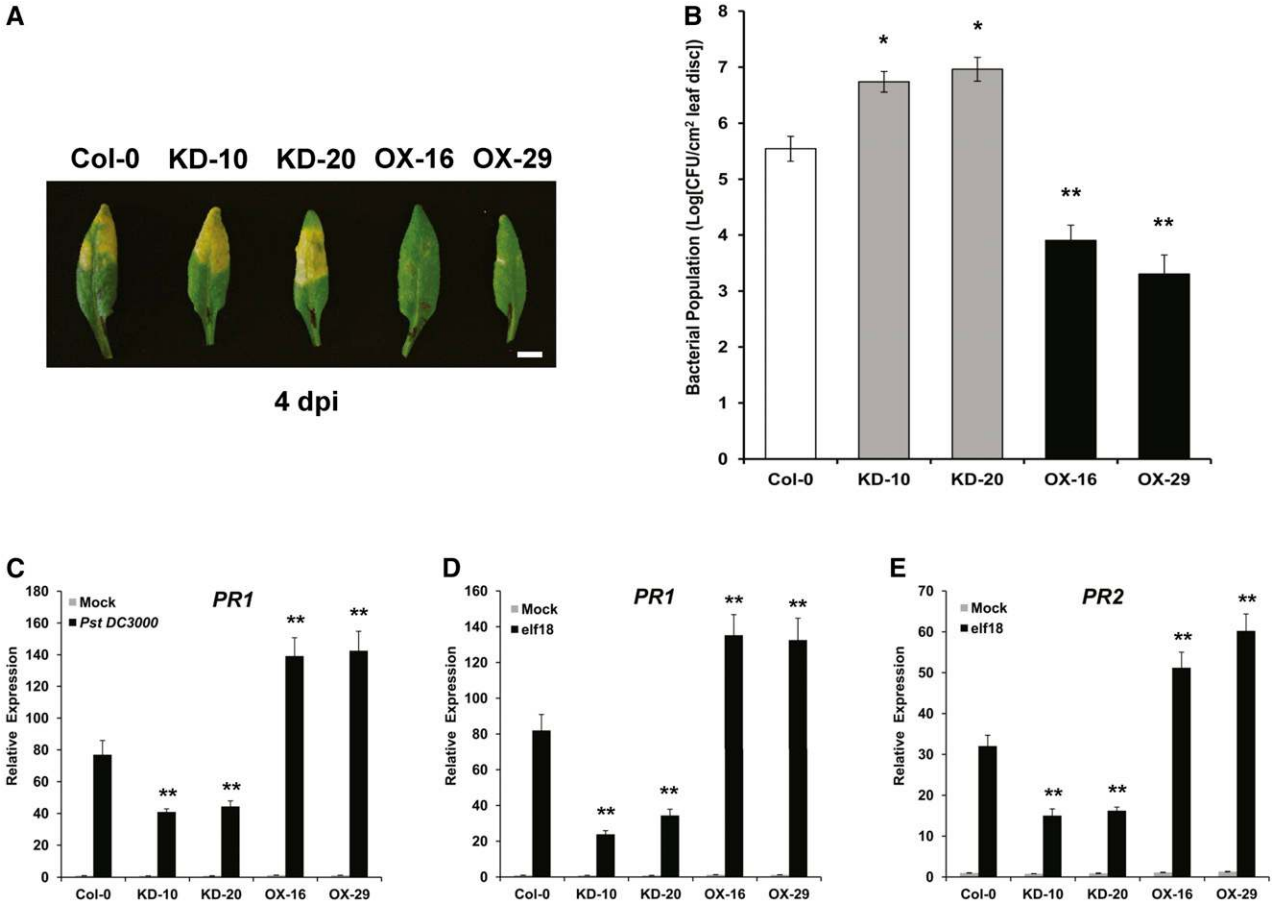

Figure 2. Defense Phenotypes of ELENA1 KD and OX Plants.

(A) Altered disease susceptibility of plants of various genotypes. Wild-type (left end), ELENA1 KD lines (#10 and #20), and ELENA1 OX lines (#16 and #29) were inoculated with *Pst* DC3000. Infected leaves were photographed at 4 d postinoculation (dpi). Bar = 5 mm.

(B) Growth of *Pst* DC3000 in plants of various genotypes. Wild-type, KD lines, and OX lines were inoculated with *Pst* DC3000 and bacterial population in each was determined at 4 d postinoculation. Bars indicate ± SD (n = 3). CFU, colony-forming units.

(C) Using qRT-PCR, *PR1* mRNA levels were determined in ELENA1 transgenic plants at 24 h after infiltration with *Pst* DC3000. Infiltration with water (gray bars) served as the mock control. All experiments were performed using 4- to 5-week-old leaf tissues and repeated at least three times with similar results.

(D) Real-time PCR analysis of *PR1* expression in the absence or presence of 5 μM elf18 for 24 h.

(E) Real-time PCR analysis of *PR2* expression in the absence or presence of 5 μM elf18 for 24 h.

For **(C)** to **(E)**, transcript levels were normalized to *ACT2* expression levels. Bars represent average ± SD (n = 3). For **(B)** to **(E)**, asterisks indicate statistically significant difference compared with the wild type (Col-0). *P < 0.05 and **P < 0.01; two-tailed t test.

et al., 2015; Nelson et al., 2016). In ELENA1 transcripts, a total of eight putative open reading frames (ORFs) are found with expected peptide lengths ranging from 2 to 43 amino acids (Supplemental Figure 3). To test whether ELENA1 functions as a noncoding or coding RNA, we generated two different mutant plants, *35S:5m_ELENA1* (ELENA1_5M) and *35S:8m_ELENA1* (ELENA1_8M). In ELENA1_5M, five start codons of putative ORFs encoding peptides longer than 10 amino acids were mutated to TTG, whereas in ELENA1_8M, every start codon of all putative ORFs was changed to TTG. Notwithstanding some differences in transcript levels (1900–2600-fold) among mutated ELENA1 OX lines, *PR1* expression was not significantly affected (Figures 3A and 3B). In the wild type, the maximal induction level of ELENA1 by elf18 is 10 to 20 times compared with the basal level (Figure 1B), but in ELENA1 OX or mutated ELENA1 OX plants, ELENA1 expression levels were over 1000 times compared with the basal level. Furthermore, we have analyzed four different OX lines with varying ELENA1 expression levels (1800–3200-fold) and found that these plants have comparable *PR1* expression levels (Supplemental Figure 2). All these results suggested that transcript levels of ELENA1 in the OX plants were already above the saturating levels for *PR1* expression, and different ELENA1 expression levels in OX plants were not expected to affect *PR1* expression level significantly.

Analyses of elf18-treated transgenic plants overexpressing the mutated ELENA1 showed increased *PR1* expression levels compared with those in wild-type plants and comparable *PR1* expression levels with WT ELENA1 OX lines (Figure 3A and 3B).

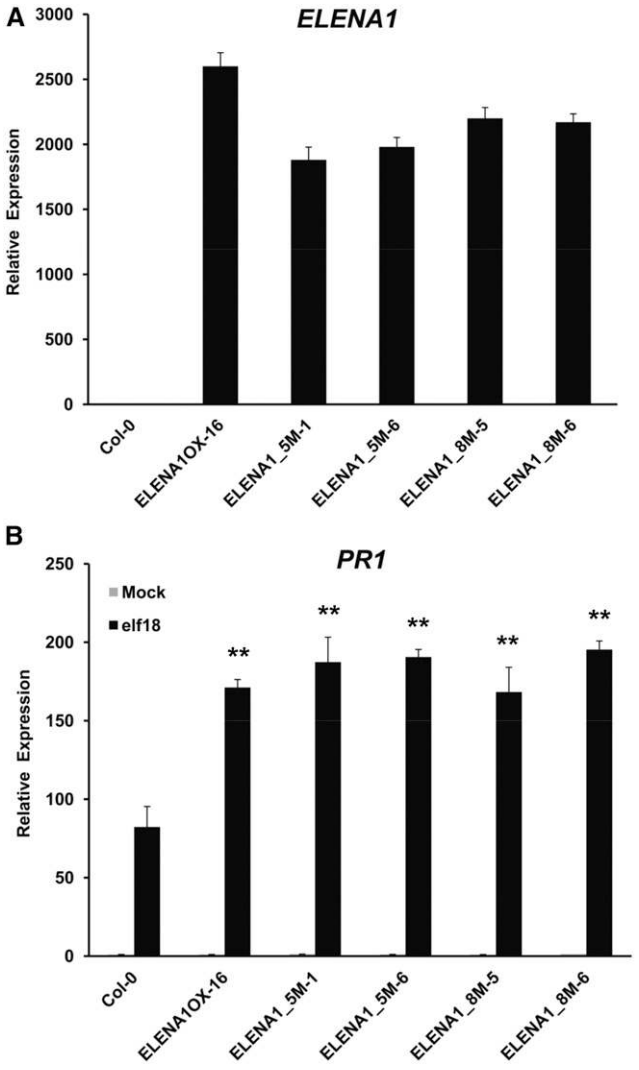

Figure 3. Elevated *PR1* Expression in Transgenic Plants Overexpressing ELENA1 Bearing Multiply Mutated Start Codons.

(A) Real-time PCR analysis of ELENA1 expression with no treatment. Both ELENA1_5M and ELENA1_8M harbor five and eight start codon mutations (ATG to TTG), respectively.

(B) Real-time PCR analysis of *PR1* expression in the absence or presence of 5 μM elf18 for 24 h. Asterisks indicate statistically significant difference compared with the wild type (Col-0). **P < 0.01; two-tailed *t* test.

For **(A)** and **(B)**, transcript levels were normalized to *ACT2* expression levels. Bars represent average ± SD (n = 3 independent seedling pools).

These results suggested that ELENA1 functions as an authentic lncRNA rather than a peptide-coding RNA.

ELENA1 Positively Regulates elf18-Induced Immune Response Genes

To investigate the role of ELENA1 in regulating the immune response, we performed strand-specific RNA-seq (ssRNA-seq) on wild-type and ELENA1 OX plants grown under normal (0 h) and elf18-treated conditions (1, 6, and 12 h; Supplemental Table 1), and three biological replicates (three independent seedling pools) were used for each condition. Clustering analysis revealed that the replicates of each condition showed gene expression profiles distinct from those of other conditions (Supplemental Figure 4A). Among 22,324 detected genes (TAIR10 annotated), 535 and 603 protein-coding genes were upregulated at all time points in wild-type and OX plants, respectively (fold change ≥ 2, P value < 0.05; Supplemental Figure 4B and Supplemental Data Sets 1 and 2). Gene Ontology (GO) enrichment analysis revealed that the functions of these genes were significantly enriched in biological processes associated with defense response and immune response (Supplemental Figure 4C), indicating that our transcriptome data sets exhibited characteristics of plants under elf18 treatment.

In addition, we confirmed that the ELENA1 transcript level was induced by elf18 because in wild-type plants, ELENA1 was upregulated in all time points following elf18 treatment (Figure 4A; Supplemental Data Set 3). In OX plants, ELENA1 expression was significantly elevated under all conditions compared with wild-type plants (Figure 4B; Supplemental Figure 4D). These results were in agreement with the above real-time PCR analysis (Figure 1B; Supplemental Figure 2).

Correlation analysis (Supplemental Figure 4A) showed that overexpression of ELENA1 did not induce global changes of gene expressions because wild-type and OX samples from the same time points were clustered together. To identify genes specifically regulated by ELENA1, we compared the transcriptomes of OX and wild-type plants under normal and elf18-treated conditions. Detailed analysis showed that the basal expression levels (under normal condition) of 95 elf18-induced (Group I) and 185 elf18-repressed genes increased and decreased, respectively, in OX plants (Figure 4C; Supplemental Data Set 4). In addition, by comparing wild-type and OX plants under elf18 treatment, we identified 145 genes with increased expression levels in OX plants compared with wild-type plants (Supplemental Data Set 4). These genes could be further classified into three additional groups. Group II contained 14 genes that had higher expression levels in all time points (Figure 4D). These genes include previously identified important regulators of defense response such as *PR1*, *PR2*, and *CRK7* (*CYSTEINE-RICH RECEPTOR-LIKE PROTEIN KINASE7*; At4g23150) (Denoux et al., 2008; Oide et al., 2013; Idänheimo et al., 2014). Group III contains 29 genes whose expression levels were increased in two time points. Representative genes of this group were *CYP82C2* (*CYTOCHROME P450, FAMILY 82, SUBFAMILY C, POLYPEPTIDE2*; At4g31970) and *BG3* (*BETA-1,3-GLUCANASE3*; At3g57240), which are known downstream defense-related genes (Dong et al., 1991; Rajniak et al., 2015). Group IV contains 102 genes that were upregulated in one time point and included some genes that have been shown to participate in defense responses, such as *PUB54* (*At1g01680*), *WRKY50* (*At5g26170*), *MYB34* (*At5g60890*), etc. (Gao et al., 2011; Frerigmann and Gigolashvili, 2014). GO enrichment analysis of these genes showed that their functions were significantly enriched in biological processes associated with systemic acquired resistance, immune responses, and defense responses (Figure 4E). Taken together, these results suggested that ELENA1 positively regulates a subset of elf18-induced defense genes.

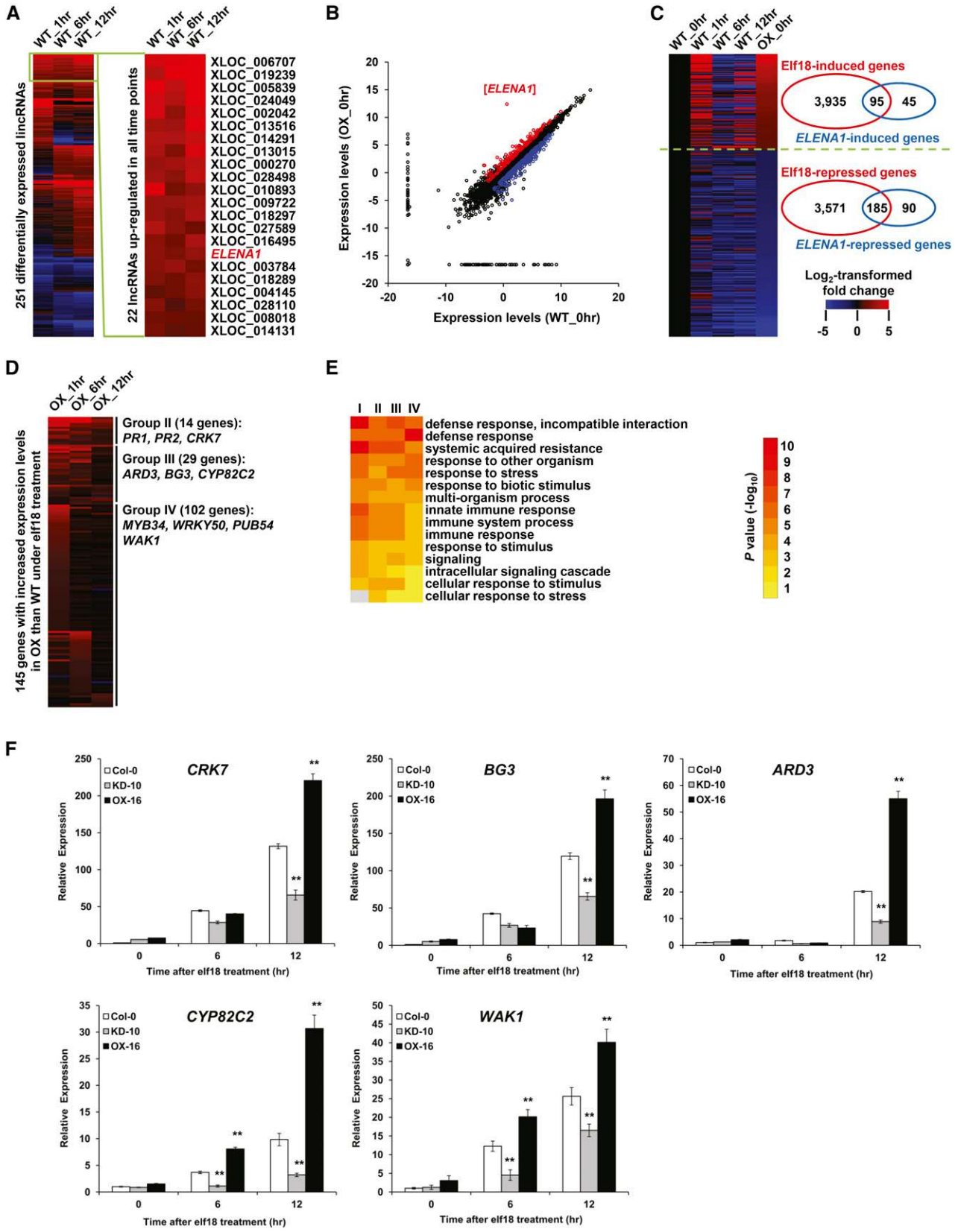

Figure 4. Transcriptional Regulation of elf18-Responsive Genes by ELENA1.

(A) Heat map showing fold changes of 251 differentially expressed lncRNAs under 5 μM elf18 treatment compared with normal condition (fold change ≥ 2 or ≤ 0.5, P value < 0.05). Twenty-two lncRNAs that were upregulated in all time points are selectively shown on the right.

We verified the expression level of selected genes in ELENA1 KD and OX lines with real-time PCR (Figure 4F). Major candidates of putative ELENA1 target genes, *PR1*, *PR2*, *CRK7*, *BG3*, and *CYP82C2*, showed a clear anticorrelation in their expression level between ELENA1 KD and OX plants. These results confirmed that ELENA1 positively regulates expression of selective defense-related genes responsive to elf18.

ELENA1 Interacts with MED19a

Lai et al. (2013) reported that lncRNA may directly associate with Mediator and promote target gene expression in human cells. However, no Mediator subunits with RNA binding motifs have been identified in Arabidopsis yet. Therefore, we examined possible direct interactions between ELENA1 and Mediator subunits. First, we screened a group of Mediator subunits with high probable RNA binding motif using BindN software (Wang and Brown, 2006). Then, we performed in vitro RNA binding assays with maltose binding protein (MBP)-tagged recombinant Mediator subunits and in vitro-transcribed ELENA1 RNA. We found that MED19a (*AT5G12230*) and MED26b (*AT5G05140*) were able to bind to ELENA1 in vitro (Supplemental Figure 5). Analyses of KO mutants of mediator subunits showed that *med19a* (*med19a-1* and *med19a-2*), not *med26b* plants, displayed a similar phenotype as ELENA1 KD lines in *PR1* expression after elf18 treatment (Supplemental Figure 6). The Arabidopsis genome contains *MED19b* (*AT5G19480*), a close homolog of MED19a. We found that ELENA1 also associated with MED19b in vitro (Supplemental Figure 7A). However, analysis of the double mutant, *MED19b* RNAi *med19a*, showed only a marginal additive effect on *PR1* expression compared with *med19a* single mutant (Supplemental Figure 8). This observation suggests that MED19a is the major regulator for *PR1* expression and MED19b played only a minor role in *PR1* expression induced by elf18. Therefore, further analysis was performed with MED19a.

Further binding competition assay with nonbiotinylated RNA confirmed that ELENA1 specifically bound to MED19a (Figures 5A and 5B). However, recombinant MED19a protein also bound to antisense ELENA1 (Supplemental Figure 7B), suggesting non-sequence-specific binding. The non-sequence-specific binding to single-stranded nucleotides (including RNA) by target proteins has been reported previously (Heo and Sung, 2011). To check the specificity of the interaction between ELENA1 and the native MED19a protein, we prepared nuclear extracts from GFP-MED19a transgenic lines to perform RNA binding assay. Contrary to in vitro binding with recombinant MED19a protein purified from *Escherichia coli*, we detected MED19a association only with the sense strand of ELENA1 (Figure 5C), demonstrating the strand-specific interaction of ELENA1 with native MED19a in vivo. We also checked in vivo association of sense ELENA1 with MED19a using trimolecular fluorescence complementation (TriFC) assay, a modified version of bimolecular fluorescence complementation (BiFC) assay using a MS2 system (Schönberger et al., 2012; Han et al., 2014). We observed that sense strand of ELENA1 associated with MED19a in the nucleus, but antisense of ELENA1 did not (Figure 5D).

We also examined in vivo association of ELENA1 with MED19a after elf18 treatment by RNA immunoprecipitation (RIP) assay using the 35S:GFP-MED19a lines. Indeed, we were able to retrieve ELENA1 from GFP-MED19a immunoprecipitates (Figure 5E); more importantly, there was an increased association of ELENA1 with MED19a specifically during elf18 treatment (Figure 5E). Taken together, these results provide further evidence that ELENA1 was specifically associated with MED19a in vivo and their association was enhanced by elf18 treatment.

ELENA1 and MED19a Are Interdependent in *PR1* Expression

To investigate the relationship between ELENA1 and MED19a in *PR1* expression, we generated four different double transgenic lines of ELENA1 and *MED19a*: *35S:ELENA1*/*med19a-1* (E1/m19a), *ELENA1* KD-10/*UBQ:MED19a* (e1#10/M19a), *ELENA1* KD-10/*med19a-1* (e1#10/m19a), and *35S:ELENA1*-16/*UBQ:MED19a* (E1#16/M19a) (Figure 6; Supplemental Figure 9). After selecting two independent lines for each double transgenic combination, we analyzed *PR1* expression with elf18 treatment. The E1/m19a lines showed greatly reduced *PR1* expression compared with ELENA1 overexpressing plant (E1#16) but showed a small increase of *PR1* expression compared with *med19a-1* mutant (m19a) (Figure 6A). This result suggested that ELENA1 function in *PR1* expression was largely dependent on MED19a, but there were factors other than MED19a associating with ELENA1 to promote *PR1* expression. ELENA1 KD mutant showed ~30% *PR1* expression levels compared with the wild type (Figure 6C). In this mutant background, knockout of MED19a (e1#10/m19a) had no further effect, indicating that MED19a action on *PR1* expression was dependent on ELENA1. This conclusion is further supported by the results of Figure 6B. In the ELENA1 KD mutant background, overexpression of MED19a (e1#10/M19a) had no significant effect on *PR1* expression, whereas in the wild-type background, overexpression of MED19a increased *PR1* expression by ~2-fold (Figure 6B). E1#16/M19a lines showed elevated *PR1* expression compared with the overexpressing plants, suggesting that ELENA1 and MED19a can interact to further enhance *PR1* expression (Figure 6D). Taken together, these results showed that under elf18 treatment, the promoting effect of MED19a on *PR1*

Figure 4. (continued).

(B) Scatterplot showing $\log_2$-transformed expression levels (FPKMs) of expressed genes in the wild type (*x* axis) compared with OX-16 plant (*y* axis).
(C) Heat map showing fold changes of 280 elf18-responsive genes with altered basal expression levels in OX plants.
(D) Heat map showing fold changes of 145 genes with increased expression levels in OX compared with wild-type plants under elf18 treatment.
(E) GO enrichment analysis of Group I, II, III, and IV genes. Top 15 (with the lowest P values) enriched GO terms of the biological process category are shown.
(F) Time-course analysis of selected target gene expression after elf18 treatment. Transcript levels were normalized to *ACT2* expression levels. Bars represent average ± SD ($n = 3$ independent seedling pools). Asterisks indicate statistically significant difference compared with the wild type (Col-0). **P < 0.01; two-tailed *t* test.

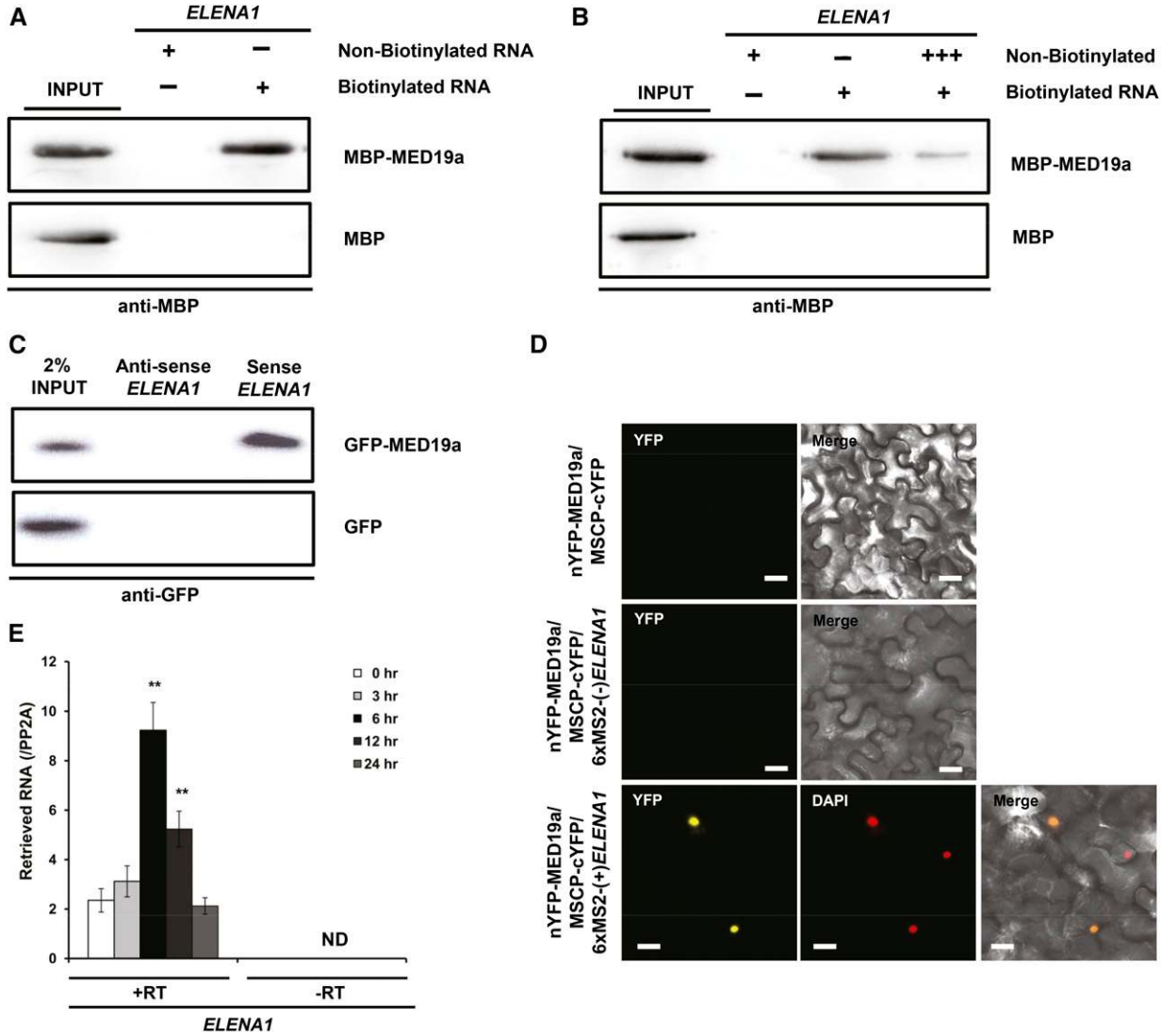

Figure 5. ELENA1 Associates with MED19a.

(A) In vitro binding assay with in vitro-transcribed biotinylated ELENA1 RNA and recombinant MBP-MED19a protein.
(B) In vitro binding competition assay with recombinant MBP-MED19a protein and in vitro-transcribed ELENA1 RNA.
(C) In vitro binding between GFP-MED19a from nuclear extracts and in vitro-transcribed sense or antisense ELENA1 RNA. GFP nuclear extracts from *35S:GFP* plants were used as a negative control.
(D) TriFC assay in tobacco leaves. nYFP was fused to MED19a, and cYFP was fused to MSCP. 6xMS2 nucleotide sequences fused to sense or antisense ELENA1. Confocal images were taken 3 d after infiltration. Bars = 20 μm.
(E) RIP assay with *35S:GFP-MED19a* line during elf18 treatment. Data (mean ± SD of qPCR; $n = 3$) are relative to the background level of RNA precipitation (*PP2A*). +RT, with reverse transcription of precipitates; –RT, without reverse transcription of precipitates. Asterisks indicate statistically significant difference compared with 0 h. **$P < 0.01$; two-tailed *t* test.
For **(A)** and **(B)**, MBP was used as a negative control. For **(C)**, *35S:GFP* was used as a negative control.

expression is dependent on ELENA1; in addition, there was a partial independent role of ELENA1 in *PR1* induction upon elf18 treatment.

ELENA1 Promotes MED19a Enrichment on the *PR1* Promoter

To investigate possible enrichment of MED19a on the *PR1* promoter, we performed chromatin immunoprecipitation (ChIP) assays with P_{MED19a}*:GFP-MED19a* transgenic line. After the ChIP assay, we quantified the enrichment of five different regions (P1 to P5) on the *PR1* promoter by qPCR (Figure 7A). MED19a enrichment on the *PR1* promoter was enhanced after elf18 treatment. MED19a enrichment was highest at 6 h after elf18 treatment and then reduced over 12 h after elf18 treatment (Figure 7B). Interestingly, MED19a enrichment was highest in the P4 region compared with other regions. Previous reports have identified a TGA binding *cis*-element, *AS-1* like, in this region

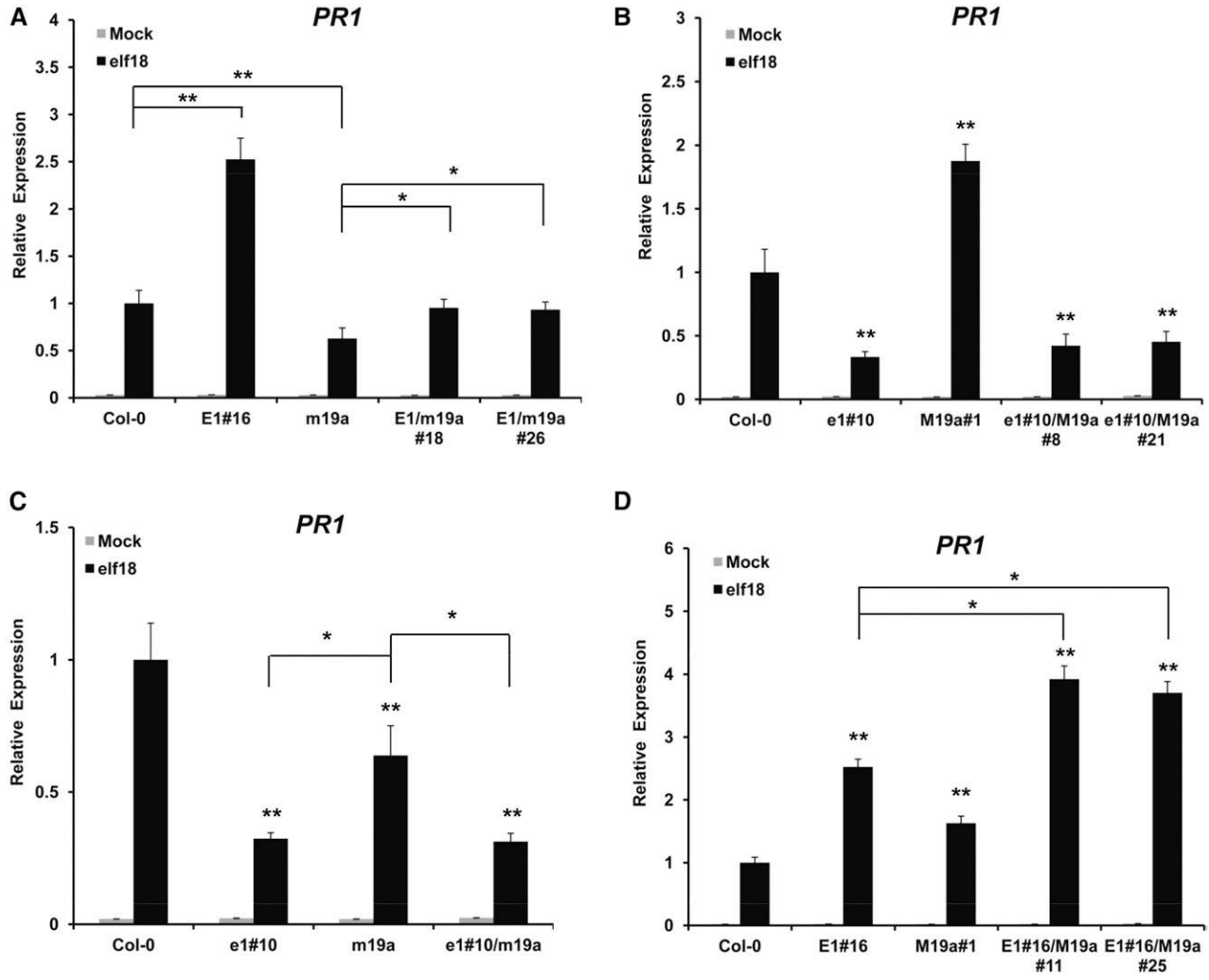

Figure 6. *PR1* Expression in ELENA1 and *MED19a* Double Mutants.

(A) *PR1* expression in *35S:ELENA1/med19a-1* (E1/m19a) plants. E1#16 is *35S:ELENA1*-16, and m19a is *med19a-1*
(B) *PR1* expression in *ELENA1* KD-10/*UBQ:MED19a* (e1#10/M19a) plants. e1#10 is *ELENA1* KD-10, and M19a#1 is *UBQ:MED19a*-1.
(C) *PR1* expression in *ELENA1 KD*-10/*med19a-1* (e1#10/m19a) plants.
(D) *PR1* expression in *35S:ELENA1*-16/*UBQ:MED19a* (E1#16/M19a) plants.
All gray bars are values for mock treatment (without elf18), and black bars are values for 12 h 5 μM elf18 treatment. Bars represent average ± SD (n = 3 independent seedling pools). Asterisks indicate statistically significant difference compared with the wild type or between indicated values. *P < 0.05 and **P < 0.01; two-tailed t test.

(Després et al., 2000; Johnson et al., 2003) (Figure 7A). This result demonstrated that MED19a was enriched on the *PR1* promoter region, especially including the TGA binding site, during elf18 treatment.

We next examined MED19a enrichment in ELENA1 mutants. In ELENA1 KD lines, the enrichment of MED19a on the P4 region of *PR1* promoter was greatly reduced compared with the wild type. On the other hand, the enrichment of MED19a in the ELENA1 OX line was increased (Figure 7C). This is consistent with elevated levels of *PR1* transcript in ELENA1 OX lines and reduced levels of *PR1* transcript in ELENA1 KD lines during elf18 treatment. These results support the view that ELENA1 facilitates the recruitment of MED19a to the *PR1* promoter.

DISCUSSION

ELENA1 Is a Positive Regulator of PTI Signaling in Arabidopsis

ELENA1 is an lncRNA induced by PAMP in plants. Like many other lncRNAs, the basal transcript level of ELENA1 was very low, but its expression level increased more than 10 times after elf18 treatment. Abolishment of ELENA1 transcriptional induction in receptor KO mutants (*efr* and *fls2*) indicated that ELENA1 transcriptional regulation was controlled by receptor-dependent signal transduction. Additionally, *ELENA1* promoter-GUS assays confirmed that its promoter carries *cis*-acting elements highly

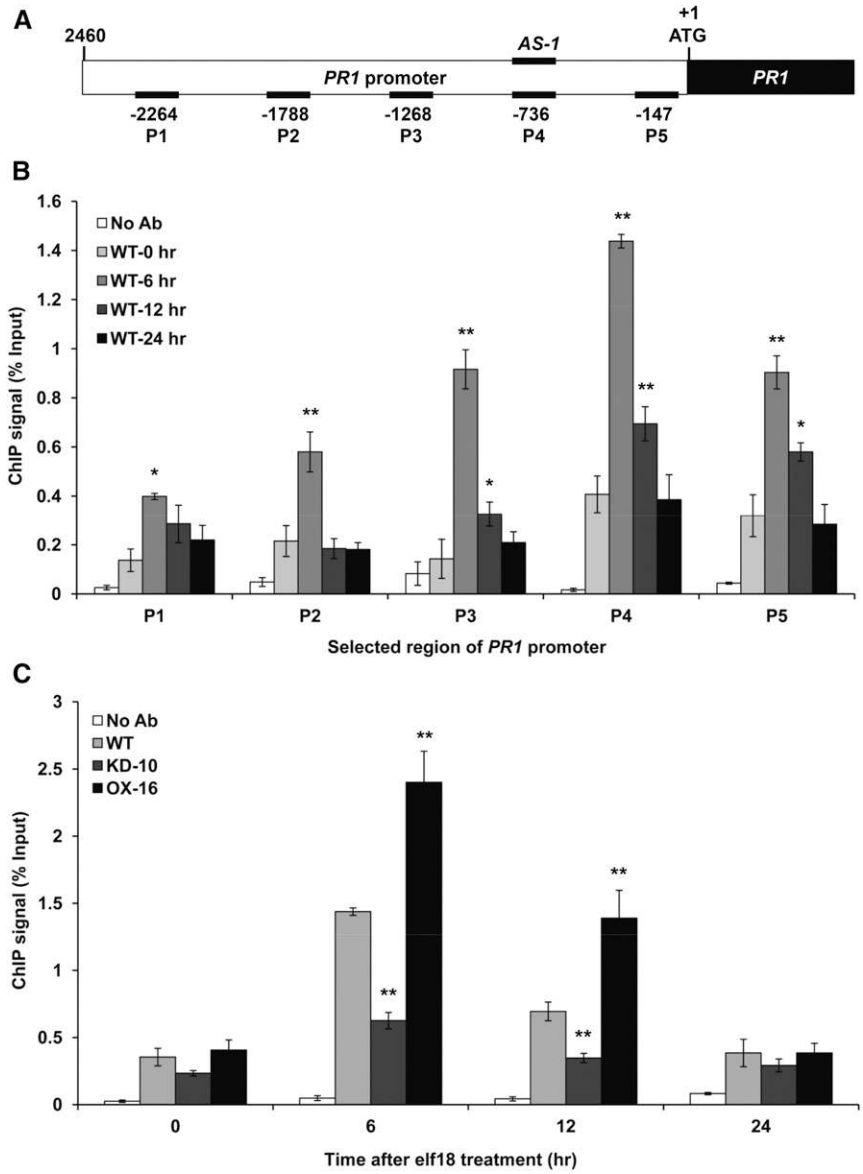

Figure 7. ELENA1 Promotes MED19a Enrichment on the *PR1* Promoter.

(A) Schematic diagrams of *PR1* promoter (2460 bp) and five different regions (P1 to P5) for analysis by ChIP assay. P4 region includes *AS-1 cis*-element.
(B) Time course of ChIP qPCR results of P_{MED19a}*:GFP-MED19a* line after elf18 treatment. ChIP signal in each region of the *PR1* promoter at each time point was quantified by qPCR. The numbers on the *x* axis indicate the positions of the PCR-amplified sites described in **(A)**.
(C) Relative enrichment of MED19a at P4 region in ELENA1 mutants (KD-10 and OX-16) was shown in different times after 5 μM elf18 treatment. Error bars indicate SD ($n = 3$). Asterisks indicate statistically significant difference compared with 0 h **(B)** and the wild type (Col-0) **(C)**. *$P < 0.05$ and **$P < 0.01$; two-tailed *t* test.

responsive to elf18 and flg22. ELENA1 is not early responsive, as its transcript level continuously increased until 12 h after elf18 or flg22 treatment. Moreover, ELENA1 expression did not respond to SA, the key hormone for systemic acquired resistance. This observation suggests that ELENA1 functions downstream of PAMP recognition and by an SA-independent signaling.

In ELENA1 KD and OX plants, the altered defense phenotypes against *Pst* DC3000 and changes in *PR1* expression after elf18 treatment clearly showed that this lncRNA served as a positive regulator of PTI signaling. RNA-seq results also demonstrated that many plant defense-related genes were upregulated in ELENA1 OX plants.

ELENA1 Transcriptionally Regulates Downstream Immune Response Genes, Including *PR1*

At the initial stage of this study, we assumed that the presumptive target genes of ELENA1 might be located in the nearby genomic

region because many lncRNAs are involved in *cis*-regulatory function (Guil and Esteller, 2012). Two genes are located close to *ELENA1*. In wild-type plants, *CBL6* but not *At4g16360* was induced by elf18 treatment (Supplemental Figure 10). Real-time qPCR and RNA-seq results of ELENA1 transgenic plants showed no difference in the transcript levels of neighboring genes including *CBL6* (Supplemental Figure 10). These results suggest that ELENA1 likely functions as a *trans*-acting lncRNA involved in the transcriptional regulation of distant target genes.

We screened candidate target genes of ELENA1 using an RNA-seq data set of ELENA1 OX line. *PR1* and *PR2* were identified as good candidates because their expression in OX lines was higher compared with the wild type at all time points after elf18 treatment. Moreover, the opposite results were obtained in ELENA1 KD mutants. We tested expression of over 30 candidate target genes screened by RNA-seq, but only a few of these genes showed a clear opposite expression pattern between ELENA1 KD mutant and OX plants. This observation suggested that ELENA1 regulates expression of only a subset of target genes.

RNA-seq and qPCR validation results showed that downstream genes, such as *PR1*, *PR2*, *BG3*, and *CYP82C2*, were major candidate ELENA1 targets, and these genes clearly showed reduced expression in KD plants but enhanced expression in OX plants. PR2 and BG3 are major β-1,3-glucanases regulating callose accumulation and SA-dependent defense responses (Oide et al., 2013). The recently characterized CYP82C2 is a biosynthetic enzyme generating a cyanogenic metabolite in Arabidopsis required for inducible pathogen defense and innate immunity (Rajniak et al., 2015). There was no difference in expression levels of early and upstream genes in PAMP signaling, e.g., *FLS2*, *EFR*, *BAK1*, *BIK1*, *PBS1*, *FRK1*, and *MAPK* genes, etc. This is not surprising because the ELENA1 transcript level increased relatively slowly and reached a maximum level between 6 and 12 h. Together, our results suggest that ELENA1 could regulate late and downstream genes rather than early-responsive upstream genes. We propose the major role of ELENA1 in PTI signaling to be enhancement of expression for specific downstream genes involved in plant innate immunity.

ELENA1 Interacts with Mediator Subunit 19a

Two notable classes of lncRNAs, activator RNAs and enhancer RNAs, regulate expression of their targets by interacting with the Mediator complex (Ørom et al., 2010; Lai et al., 2013; Allen and Taatjes, 2015). Inspired by these findings, we examined possible interactions of ELENA1 with selected Mediator subunits carrying a putative RNA binding motif and found that ELENA1 binds to MED19a and MED26b in vitro. However, each mediator KO mutant showed different *PR1* gene expression pattern upon elf18 treatment (Supplemental Figure 6). These results raised the possibility that ELENA1 could bind to different sets of Mediator subunits in vivo depending on the signals.

A recent report showed that the fungal effector (HaRxL44) of powdery mildew mediates proteasome-dependent degradation of MED19a and shifts the balance from SA-mediated disease resistance to ethylene/jasmonic acid-mediated transcriptomic changes (Caillaud et al., 2013). This result suggests that MED19a plays an important role in biotrophic pathogen resistance and could be involved in PTI signaling. Our result on *PR1* expression in MED19a KO mutants after elf18 treatment also supported this view. Analysis of double mutants of ELENA1 and *MED19a* showed that the function of MED19a in *PR1* expression is closely related to ELENA1. Our results also suggested that ELENA1 can partially promote *PR1* expression in a MED19a-independent way (Figure 6). There are two possible explanations for this. First, ELENA1 may bind to other Mediator subunits and partially regulate *PR1* expression. We have already shown the possibility that ELENA1 can bind to other Mediator subunits (Supplemental Figure 5). Second, the MED19a homolog, MED19b, also associates with ELENA1 and the complex may regulate *PR1* gene expression (Supplemental Figures 7A and 8). In Supplemental Figure 8, we showed that MED19b might play a minor role by interacting with ELENA1 and affect *PR1* expression. Therefore, the slightly higher expression of *PR1* in E1/m19a compared with that in the *med19a* single mutant may be caused by MED19b. The e1#10/M19a plants showed almost similar *PR1* expression levels as the single ELENA1 KD line because ELENA1 was almost depleted in the e1#10/M19a mutant (Figure 6B). In Figure 6C, the *PR1* expression level in *med19a-1* was higher than that in the ELENA1 KD plants. Also, the *PR1* expression level in the e1#10/m19a line was similar to that in the ELENA1 KD line because ELENA1 expression was already depleted. These observations suggested that MED19b might have redundant function with MED19a. Therefore, all these lines of evidence supported the notion that ELENA1 affects transcription of defense-related target genes through Mediator subunits, including MED19a.

ELENA1 Regulates MED19a Enrichment on the *PR1* Promoter

Analysis of transgenic plants with different genotypes of ELENA1 and *MED19a* suggested that ELENA1 and MED19a were interdependent for *PR1* expression induced by elf18 treatment. However, it was not clear whether ELENA1 and MED19a regulate *PR1* gene expression directly or indirectly. ChIP-PCR analysis clearly showed that MED19a was enriched on the *AS-1*-like element-containing region of *PR1* promoter. Decreased MED19a enrichment in ELENA1 KD lines and increased MED19a enrichment in ELENA1 OX lines on the *PR1* promoter demonstrated that ELENA1 facilitated MED19a enrichment on the *PR1* promoter (Supplemental Figure 11). In addition, it was reported that multiple TGA factors have a binding capacity for both positive and negative regulatory *AS-1*-like *cis*-elements present on the *PR1* promoter (Jupin and Chua, 1996; Després et al., 2000; Pajerowska-Mukhtar et al., 2013). This suggested that transcriptional regulation of *PR1* by ELENA1 and MED19a might be closely related with TGA TFs.

Notwithstanding our results, the detailed mechanism of MED19a enrichment on the *PR1* promoter by ELENA1 remains to be clarified. Several mechanisms have been proposed for the involvement of *trans*-acting lncRNA in transcriptional regulation of target genes (Koziol and Rinn, 2010; Vance and Ponting, 2014). One possible model is Triple helix formation between ELENA1 lncRNA and *PR1* promoter DNA. Using Triplexator software (Buske et al., 2012), we were unable to find any significant sequence area for triple helix formation between ELENA1 and *PR1* promoter sequences. Another possible model is that ELENA1 may interact with other proteins, such as other Mediator subunits, transcription factors, cofactors, or adaptors, thereby recruiting

MED19a to the transcription machinery. In this regard, we have shown that ELENA1 could bind to another mediator, MED26b. It is possible that ELENA1 can bind to other Mediator subunits and other transcriptional machinery components. Further study of other interactors will likely provide additional information of the regulatory complexity of this noncoding RNA.

The roles of lncRNA in plant immunity are only beginning to be unraveled. In addition to ELENA1, our custom lncRNA array and RNA-seq data have uncovered hundreds of lncRNAs that are upregulated or downregulated by elf18 treatment, suggesting that many lncRNAs may be involved in the regulation of plant innate immunity. We anticipate that further studies of other lncRNAs may lead to a better understanding of the roles of lncRNAs in transcriptome regulation associated with plant immunity.

METHODS

Plant Materials, Growth Conditions, and Treatment

Arabidopsis thaliana ecotype Columbia (Col-0), *efr-2* (SALK_068675), *fls2* (SALK_062054), *med19a-1* (SALK_037435), *med19a-2* (SALK_034955), and *med26b-1* (SALK_020870) mutant plants were used. T-DNA insertion lines were obtained from the SALK collection. Homozygous plants for the T-DNA insertion were selected by genotyping progeny plants according to Alonso et al. (2003). Absence of target gene expression in homozygous plants was further confirmed by RT-PCR. Plants of all genotypes were grown on 0.6% agar media containing 0.5× Murashige and Skoog (MS) salts (MP Biomedicals), 1% sucrose (Fisher), and 0.5 g/L MES hydrate (Sigma-Aldrich) in a growth room at 22°C under 16 h light/8 h dark with white fluorescent light (~100 μmol m^{-2} s^{-1}). For elf18 (EZBiolab) or flg22 (EZBiolab) treatment, 10-d-old seedlings grown on MS solid medium were transferred to MS liquid medium (pH 5.7) with 1% sucrose and 5 μM elf18 or flg22 and incubated under the same condition and then seedlings were harvested at each time point after peptide application.

Generation of Transgenic Lines

The entry clone of ELENA1 was recombined into pBA-DC (Zhang et al., 2005) to generate overexpressing plants. ELENA1 KD mutants were generated using artificial microRNA (Niu et al., 2006). To produce ELENA1 codon mutants, we made an entry clone of full-length mutated ELENA1 by DNA synthesis (IDT) and recombined entry clone into pBA-DC by LR reaction. The E1/m19a lines were generated by transforming the *med19a-1* knockout mutant with *pBA-ELENA1*. The e1#10/M19a line were generated by transforming ELENA1 KD-10 with *pUBQ-MED19a*. The e1#10/m19a lines were produced by genetic crossing between ELENA1 KD-10 and *med19a-1* knockout mutant. The E1#16/M19a lines were generated by transforming ELENA1 OX-16 with *pUBQ-MED19a*. P_{MED19a}*:GFP-MED19a* mutants were generated with pKGWFS7 vector (Karimi et al., 2002). All constructs were verified by sequencing and transformed into *Agrobacterium tumefaciens* strain GV3101. Wild-type (Col-0) or mutant plants were transformed using the floral dip method (Zhang et al., 2006).

Real-Time RT-PCR Analysis

Total RNA was extracted from Arabidopsis seedlings using RNeasy plant mini kit (Qiagen) including DNase I treatment. Reverse transcription was performed using 2 μg of each total RNA and oligo$(dT)_{20}$ primers by the SuperScript III reverse transcriptase (Invitrogen). Real-time RT-PCR was performed using SYBR premix Ex Taq (Tli RNaseH plus; TaKaRa) on the Bio-Rad CFX96 real-time system with gene-specific primers. Primer sequences used are listed in Supplemental Table 2.

Histochemical GUS Staining

For promoter-GUS fusion, two promoter fragments of ELENA1 (200 and 1500 bp) were amplified by PCR, cloned into pENTR/D-TOPO vector (Invitrogen), and then recombined into pKGWFS7 vector to obtain the P_{200}*:GUS* and P_{1500}*:GUS* fusions. Arabidopsis (Col-0) plants were transformed by the floral dip method and GUS staining was performed as described (Senecoff et al., 1996).

Bacterial Growth Assays

Bacterial growth assays were performed as described (Katagiri et al., 2002) with minor modifications. For leaf assay, an overnight culture of *Pseudomonas syringae* pv *tomato* DC3000 was collected by centrifugation, washed, and then resuspended to 5×10^4 colony-forming units/mL in water. Arabidopsis leaves of 4-week-old plants were infiltrated with bacterial suspension using a needleless syringe. Four days after infiltration, leaf disks were ground in 100 μL water, and serial dilutions were plated on King's B medium. Bacterial colony-forming units were counted 2 d after incubation at 28°C.

RNA Extraction, Library Construction, and Sequencing for ssRNA-Seq

Total RNA was extracted from Arabidopsis 10-d-old seedlings using TRIzol reagent (Ambion), treated with TURBO DNase (Ambion), and purified using RNeasy mini spin column (Qiagen). The quality of purified RNA was assessed using an Agilent 2100 Bioanalyzer. cDNA libraries for ssRNA-seq were prepared using the Illumina TruSeq Stranded mRNA sample preparation kit according to the low sample protocol guidelines. The quality and size of each sample library was assessed using an Agilent High Sensitivity D1K ScreenTape System. The average sizes of the enriched cDNA fragments were between 272 and 300 bp. The three biological replicates for each condition (negative control, 1 h_elf18, 6 h_elf18, and 12 h_elf18) were pooled into one well and sequenced on an Illumina NextSeq High Output SR 75 with 75-cycle single reads per multiplexed sample.

ssRNA-Seq Data Analysis

Strand-specific RNA-seq reads were mapped to the Arabidopsis genome (TAIR10) using TopHat (version 2.0.8) (Kim et al., 2013) with parameters "–library-type=fr-firststrand -i 40 -I 5000 -g 1–segment-length=20." The mapped reads were assembled using Cufflinks (v2.1.1) (Trapnell et al., 2013) with parameters "–library-type=fr-firststrand -I 5000–min-intron-length=40" and with TAIR10 annotation as the reference (Lamesch et al., 2012). The assembled transcripts of each ssRNA-seq sample were merged and annotated using Cuffcompare (v2.1.1) (Trapnell et al., 2013) with TAIR10 annotations as the reference. The expression level of each gene was then calculated by fragments per kilobase of exons per million fragments mapped (FPKM) using Cuffdiff (v2.1.1) (Trapnell et al., 2013) with parameter "–library-type=fr-firststrand." A 2-fold variance in FPKM, a P value < 0.05, and an adjusted P value < 0.1 were used as cutoffs to define differentially expressed genes. The P value and adjusted P value were calculated using DESeq2 (Love et al., 2014). All assembled intergenic transcription units were collected as lncRNA candidates. Candidate genes encoding RNA with length ≥200 nucleotides and a predicted ORF ≤100 amino acids were defined as lncRNA (Liu et al., 2012). ORFs were predicted using GenScan with Arabidopsis specific parameters (Burge and Karlin, 1997). GO enrichment analysis was performed using agriGO (Du et al., 2010) with TAIR10 annotation. The smaller the P value is, the more the GO term is significantly enriched; therefore, the top enriched GO terms are those with the smallest P values.

In Vitro RNA Pull-Down Assay and RIP Assay

Biotin-labeled RNAs were in vitro transcribed using the Biotin RNA Labeling Mix (Roche) and T7 RNA polymerase (Roche), treated with RNase-free DNase I (Invitrogen), and purified with RNeasy Mini Kit (Qiagen). Nuclear extract was obtained from seedling samples as described (Heo and Sung, 2011). In addition, recombinant MBP-Mediator subunit proteins were expressed with pMAL-DC and purified using *Escherichia coli* (BL21) expression system. Two micrograms of biotin-labeled RNAs and nuclear extract from GFP-MED19a transgenic plants or recombinant Mediator proteins were mixed in pull-down buffer (50 mM Tris, pH 7.5, 150 mM NaCl, 2 mM DTT, 0.05% Nonidet P-40, and protease inhibitor tablet [Roche]) and incubated for 6 h at 4°C. Thirty microliters of washed streptavidin agarose beads (Roche) were then added to each binding reaction and further incubated for 2 h at 4°C. Beads were washed briefly five times using binding buffer and boiled in SDS buffer, and the supernatant was analyzed by protein gel blot using anti-GFP antibody (Santa Cruz). RIP assay with GFP-MED19a line was performed as previously described (Heo and Sung, 2011)

TriFC Assay

We generated binary gateway BiFC vectors, pBA3136, pBA3134, pBA3132, and pBA3130, by recombining pBA002 binary vector with Gateway cassettes of BiFC vectors, pSAT4-DEST-nEYFP-C1(pE3136), pSAT4(A)-DEST-nEYFP-N1(pE3134), pSAT5-DEST-cEYFP-C1(pE3132), and pSAT5(A)-DEST-cEYFP-N1(pE3130) (ABRC) for transient assay in *Nicotiana benthamiana*. In the case of TriFC assay, full-length entry clone carrying *MED19a* was recombined into pBA3136, and entry clone encoding MSCP was recombined into pBA3132 by LR reaction. Entry clone of *ELENA1* was recombined into p35S-GW-6xMS2 by LR reaction (Schönberger et al., 2012). All constructs were transformed into Agrobacterium strain GV3101 using the freeze and thaw method. Cultured cells were harvested and resuspended in 10 mM $MgCl_2$ plus 150 μM acetosyringone (Sigma-Aldrich) and then kept at 25°C for at least 3 h without shaking. Agrobacterium suspensions containing 50 μM MG132 were infiltrated into leaves of *N. benthamiana* with a needleless syringe. Leaf cells were analyzed using LSM 780 confocal laser scanning microscope (Zeiss) 2 to 3 d after infiltration.

ChIP Assay

ChIP assays were performed as described previously (Bowler et al., 2004). After chromatin isolation, immunoprecipitation was performed using anti-GFP (Santa Cruz). Cross-links were reversed by incubation at 65°C for 12 h, and DNA was purified with QIAquick spin columns (Qiagen) and eluted in 50 μL of Tris-EDTA buffer (pH 8.0). Real-time qPCR was used to quantify the enrichment of different fragments on the *PR1* promoter. First, relative enrichment of each fragment was calculated based on comparison to qPCR using input control. Second, relative enrichment was calculated by comparison to control region. Real-time PCR reaction was performed on Bio-Rad CFX96 real-time system. Primer sequences are in Supplemental Table 2.

Accession Numbers

Sequence data from this article can be found in the Arabidopsis Genome Initiative or GenBank/EMBL databases under the following accession numbers: ELENA1 (At4g16355), CALCINEURIN B-LIKE6 (At4g16350), PR1 (At2g14610), PR2 (At3g57260), FLS2 (At5g46330), EFR (At5g20480), PUB54 (At1g01680), WRKY50 (At5g26170), MYB34 (At5g60890), MED19a (AT5G12230), MED19b (AT5G19480), and MED26b (AT5G05140). A total of 24 ssRNA-seq data sets generated in this work have been deposited in the NCBI Gene Expression Omnibus database under accession number GSE93560 (https://www.ncbi.nlm.nih.gov/geo/query/acc.cgi?token=abehwqeihnsrzohandacc=GSE93560).

Supplemental Data

Supplemental Figure 1. Expression level of selected ELENA1 knock down lines by artificial miRNA.

Supplemental Figure 2. ELENA1 and *PR1* expression level in selected ELENA1-overexpressing lines.

Supplemental Figure 3. Predicted ORFs in ELENA1 transcript.

Supplemental Figure 4. Global view of ssRNA-seq results.

Supplemental Figure 5. ELENA1 associates with Mediator subunits in vitro.

Supplemental Figure 6. *PR1* expression levels in *MED19a* and *MED26a* KO mutants after elf18 treatment.

Supplemental Figure 7. ELENA1 associates with both MED19a and MED19b in vitro.

Supplemental Figure 8. *PR1* expression levels in *med19a/med19b* double mutant plants.

Supplemental Figure 9. ELENA1 and *MED19a* expression levels in ELENA1 and MED19a double mutants.

Supplemental Figure 10. Time-course expression of genes neighboring ELENA1 after elf18 treatment.

Supplemental Figure 11. A working model of transcriptional regulation of *PR1* by ELENA1 in Arabidopsis.

Supplemental Table 1. Statistics of ssRNA-seq reads that could map to the Arabidopsis genome.

Supplemental Table 2. Primers used in this study.

Supplemental Data Set 1. Tabulated data of gene expression levels detected by ssRNA-seq.

Supplemental Data Set 2. Tabulated data of gene expression levels of 535 and 603 protein coding genes that were upregulated at all time points in wild-type and OX plants.

Supplemental Data Set 3. Tabulated data of gene expression levels of 251 differentially expressed lncRNAs.

Supplemental Data Set 4. Tabulated data of gene expression levels of upregulated genes in OX plants.

ACKNOWLEDGMENTS

We thank Fumiaki Katagiri for *Pst* DC3000 strain and Jonathan D.G. Jones for *MED19a* KO and OX seeds. This work was funded in part by Singapore NRF RSSS Grant NRF-RSSS-002.

AUTHOR CONTRIBUTIONS

J.S.S., C.J., and N.-H.C. conceived the research plans. J.S.S. and N.-H.C. designed the experiments. J.S.S., B.S.P., and C.-H.H. performed the experiments. H.-X.S. analyzed the RNA-seq data. J.S.S., H.-X.S., C.J., S.-D.Y., and N.-H.C. wrote the article.

Received December 1, 2016; revised March 7, 2017; accepted April 7, 2017; published April 11, 2017.

REFERENCES

Allen, B.L., and Taatjes, D.J. (2015). The Mediator complex: a central integrator of transcription. Nat. Rev. Mol. Cell Biol. **16:** 155–166.

Alonso, J.M., et al. (2003). Genome-wide insertional mutagenesis of *Arabidopsis thaliana*. Science **301:** 653–657.

Anderson, D.M., Anderson, K.M., Chang, C.L., Makarewich, C.A., Nelson, B.R., McAnally, J.R., Kasaragod, P., Shelton, J.M., Liou, J., Bassel-Duby, R., and Olson, E.N. (2015). A micropeptide encoded by a putative long noncoding RNA regulates muscle performance. Cell **160:** 595–606.

Ariel, F., Jegu, T., Latrasse, D., Romero-Barrios, N., Christ, A., Benhamed, M., and Crespi, M. (2014). Noncoding transcription by alternative RNA polymerases dynamically regulates an auxin-driven chromatin loop. Mol. Cell **55:** 383–396.

Bardou, F., Ariel, F., Simpson, C.G., Romero-Barrios, N., Laporte, P., Balzergue, S., Brown, J.W., and Crespi, M. (2014). Long noncoding RNA modulates alternative splicing regulators in Arabidopsis. Dev. Cell **30:** 166–176.

Bednarek, P. (2012). Chemical warfare or modulators of defence responses - the function of secondary metabolites in plant immunity. Curr. Opin. Plant Biol. **15:** 407–414.

Boller, T., and Felix, G. (2009). A renaissance of elicitors: perception of microbe-associated molecular patterns and danger signals by pattern-recognition receptors. Annu. Rev. Plant Biol. **60:** 379–406.

Bowler, C., Benvenuto, G., Laflamme, P., Molino, D., Probst, A.V., Tariq, M., and Paszkowski, J. (2004). Chromatin techniques for plant cells. Plant J. **39:** 776–789.

Burge, C., and Karlin, S. (1997). Prediction of complete gene structures in human genomic DNA. J. Mol. Biol. **268:** 78–94.

Buske, F.A., Bauer, D.C., Mattick, J.S., and Bailey, T.L. (2012). Triplexator: detecting nucleic acid triple helices in genomic and transcriptomic data. Genome Res. **22:** 1372–1381.

Caillaud, M.C., Asai, S., Rallapalli, G., Piquerez, S., Fabro, G., and Jones, J.D. (2013). A downy mildew effector attenuates salicylic acid-triggered immunity in Arabidopsis by interacting with the host mediator complex. PLoS Biol. **11:** e1001732.

Chekanova, J.A., et al. (2007). Genome-wide high-resolution mapping of exosome substrates reveals hidden features in the Arabidopsis transcriptome. Cell **131:** 1340–1353.

Denoux, C., Galletti, R., Mammarella, N., Gopalan, S., Werck, D., De Lorenzo, G., Ferrari, S., Ausubel, F.M., and Dewdney, J. (2008). Activation of defense response pathways by OGs and Flg22 elicitors in Arabidopsis seedlings. Mol. Plant **1:** 423–445.

Després, C., DeLong, C., Glaze, S., Liu, E., and Fobert, P.R. (2000). The Arabidopsis NPR1/NIM1 protein enhances the DNA binding activity of a subgroup of the TGA family of bZIP transcription factors. Plant Cell **12:** 279–290.

Dong, X., Mindrinos, M., Davis, K.R., and Ausubel, F.M. (1991). Induction of Arabidopsis defense genes by virulent and avirulent *Pseudomonas syringae* strains and by a cloned avirulence gene. Plant Cell **3:** 61–72.

Du, Z., Zhou, X., Ling, Y., Zhang, Z., and Su, Z. (2010). agriGO: a GO analysis toolkit for the agricultural community. Nucleic Acids Res. **38:** W64–W70.

Eulgem, T., and Somssich, I.E. (2007). Networks of WRKY transcription factors in defense signaling. Curr. Opin. Plant Biol. **10:** 366–371.

Franco-Zorrilla, J.M., Valli, A., Todesco, M., Mateos, I., Puga, M.I., Rubio-Somoza, I., Leyva, A., Weigel, D., García, J.A., and Paz-Ares, J. (2007). Target mimicry provides a new mechanism for regulation of microRNA activity. Nat. Genet. **39:** 1033–1037.

Frerigmann, H., and Gigolashvili, T. (2014). MYB34, MYB51, and MYB122 distinctly regulate indolic glucosinolate biosynthesis in *Arabidopsis thaliana*. Mol. Plant **7:** 814–828.

Gao, Q.M., Venugopal, S., Navarre, D., and Kachroo, A. (2011). Low oleic acid-derived repression of jasmonic acid-inducible defense responses requires the WRKY50 and WRKY51 proteins. Plant Physiol. **155:** 464–476.

Gatz, C. (2013). From pioneers to team players: TGA transcription factors provide a molecular link between different stress pathways. Mol. Plant Microbe Interact. **26:** 151–159.

Gómez-Gómez, L., and Boller, T. (2000). FLS2: an LRR receptor-like kinase involved in the perception of the bacterial elicitor flagellin in Arabidopsis. Mol. Cell **5:** 1003–1011.

Guil, S., and Esteller, M. (2012). Cis-acting noncoding RNAs: friends and foes. Nat. Struct. Mol. Biol. **19:** 1068–1075.

Guttman, M., et al. (2009). Chromatin signature reveals over a thousand highly conserved large non-coding RNAs in mammals. Nature **458:** 223–227.

Han, Y., Wang, S., Zhang, Z., Ma, X., Li, W., Zhang, X., Deng, J., Wei, H., Li, Z., Zhang, X.E., and Cui, Z. (2014). In vivo imaging of protein-protein and RNA-protein interactions using novel far-red fluorescence complementation systems. Nucleic Acids Res. **42:** e103.

Heo, J.B., and Sung, S. (2011). Vernalization-mediated epigenetic silencing by a long intronic noncoding RNA. Science **331:** 76–79.

Idänheimo, N., Gauthier, A., Salojärvi, J., Siligato, R., Brosché, M., Kollist, H., Mähönen, A.P., Kangasjärvi, J., and Wrzaczek, M. (2014). The Arabidopsis thaliana cysteine-rich receptor-like kinases CRK6 and CRK7 protect against apoplastic oxidative stress. Biochem. Biophys. Res. Commun. **445:** 457–462.

Johnson, C., Boden, E., and Arias, J. (2003). Salicylic acid and NPR1 induce the recruitment of trans-activating TGA factors to a defense gene promoter in Arabidopsis. Plant Cell **15:** 1846–1858.

Jones, J.D., and Dangl, J.L. (2006). The plant immune system. Nature **444:** 323–329.

Jupin, I., and Chua, N.H. (1996). Activation of the CaMV as-1 cis-element by salicylic acid: differential DNA-binding of a factor related to TGA1a. EMBO J. **15:** 5679–5689.

Kapranov, P., Willingham, A.T., and Gingeras, T.R. (2007). Genome-wide transcription and the implications for genomic organization. Nat. Rev. Genet. **8:** 413–423.

Karimi, M., Inzé, D., and Depicker, A. (2002). GATEWAY vectors for Agrobacterium-mediated plant transformation. Trends Plant Sci. **7:** 193–195.

Katagiri, F., Thilmony, R., and He, S.Y. (2002). The *Arabidopsis thaliana-Pseudomonas syringae* interaction. Arabidopsis Book **1:** e0039.

Kesarwani, M., Yoo, J., and Dong, X. (2007). Genetic interactions of TGA transcription factors in the regulation of pathogenesis-related genes and disease resistance in Arabidopsis. Plant Physiol. **144:** 336–346.

Kim, D., Pertea, G., Trapnell, C., Pimentel, H., Kelley, R., and Salzberg, S.L. (2013). TopHat2: accurate alignment of transcriptomes in the presence of insertions, deletions and gene fusions. Genome Biol. **14:** R36.

Koziol, M.J., and Rinn, J.L. (2010). RNA traffic control of chromatin complexes. Curr. Opin. Genet. Dev. **20:** 142–148.

Kung, J.T., Colognori, D., and Lee, J.T. (2013). Long noncoding RNAs: past, present, and future. Genetics **193:** 651–669.

Kunze, G., Zipfel, C., Robatzek, S., Niehaus, K., Boller, T., and Felix, G. (2004). The N terminus of bacterial elongation factor Tu elicits innate immunity in Arabidopsis plants. Plant Cell **16:** 3496–3507.

Lai, F., Orom, U.A., Cesaroni, M., Beringer, M., Taatjes, D.J., Blobel, G.A., and Shiekhattar, R. (2013). Activating RNAs associate with Mediator to enhance chromatin architecture and transcription. Nature **494:** 497–501.

Lamesch, P., et al. (2012). The Arabidopsis Information Resource (TAIR): improved gene annotation and new tools. Nucleic Acids Res. **40:** D1202–D1210.

Liu, J., Wang, H., and Chua, N.H. (2015). Long noncoding RNA transcriptome of plants. Plant Biotechnol. J. **13:** 319–328.

Liu, J., Jung, C., Xu, J., Wang, H., Deng, S., Bernad, L., Arenas-Huertero, C., and Chua, N.H. (2012). Genome-wide analysis uncovers regulation of long intergenic noncoding RNAs in Arabidopsis. Plant Cell **24:** 4333–4345.

Love, M.I., Huber, W., and Anders, S. (2014). Moderated estimation of fold change and dispersion for RNA-seq data with DESeq2. Genome Biol. **15:** 550.

Nelson, B.R., et al. (2016). A peptide encoded by a transcript annotated as long noncoding RNA enhances SERCA activity in muscle. Science **351:** 271–275.

Niu, Q.W., Lin, S.S., Reyes, J.L., Chen, K.C., Wu, H.W., Yeh, S.D., and Chua, N.H. (2006). Expression of artificial microRNAs in transgenic *Arabidopsis thaliana* confers virus resistance. Nat. Biotechnol. **24:** 1420–1428.

Oide, S., Bejai, S., Staal, J., Guan, N., Kaliff, M., and Dixelius, C. (2013). A novel role of PR2 in abscisic acid (ABA) mediated, pathogen-induced callose deposition in *Arabidopsis thaliana*. New Phytol. **200:** 1187–1199.

Ørom, U.A., Derrien, T., Beringer, M., Gumireddy, K., Gardini, A., Bussotti, G., Lai, F., Zytnicki, M., Notredame, C., Huang, Q., Guigo, R., and Shiekhattar, R. (2010). Long noncoding RNAs with enhancer-like function in human cells. Cell **143:** 46–58.

Pajerowska-Mukhtar, K.M., Emerine, D.K., and Mukhtar, M.S. (2013). Tell me more: roles of NPRs in plant immunity. Trends Plant Sci. **18:** 402–411.

Rajniak, J., Barco, B., Clay, N.K., and Sattely, E.S. (2015). A new cyanogenic metabolite in Arabidopsis required for inducible pathogen defence. Nature **525:** 376–379.

Rinn, J.L., and Chang, H.Y. (2012). Genome regulation by long noncoding RNAs. Annu. Rev. Biochem. **81:** 145–166.

Samanta, S., and Thakur, J.K. (2015). Importance of Mediator complex in the regulation and integration of diverse signaling pathways in plants. Front. Plant Sci. **6:** 757.

Schönberger, J., Hammes, U.Z., and Dresselhaus, T. (2012). In vivo visualization of RNA in plants cells using the λN_{22} system and a GATEWAY-compatible vector series for candidate RNAs. Plant J. **71:** 173–181.

Senecoff, J.F., McKinney, E.C., and Meagher, R.B. (1996). De novo purine synthesis in *Arabidopsis thaliana*. II. The PUR7 gene encoding 5′-phosphoribosyl-4-(N-succinocarboxamide)-5-aminoimidazole synthetase is expressed in rapidly dividing tissues. Plant Physiol. **112:** 905–917.

St Laurent, G., Wahlestedt, C., and Kapranov, P. (2015). The landscape of long noncoding RNA classification. Trends Genet. **31:** 239–251.

Swiezewski, S., Liu, F., Magusin, A., and Dean, C. (2009). Cold-induced silencing by long antisense transcripts of an Arabidopsis Polycomb target. Nature **462:** 799–802.

Trapnell, C., Hendrickson, D.G., Sauvageau, M., Goff, L., Rinn, J.L., and Pachter, L. (2013). Differential analysis of gene regulation at transcript resolution with RNA-seq. Nat. Biotechnol. **31:** 46–53.

Vance, K.W., and Ponting, C.P. (2014). Transcriptional regulatory functions of nuclear long noncoding RNAs. Trends Genet. **30:** 348–355.

van Loon, L.C., Rep, M., and Pieterse, C.M. (2006). Significance of inducible defense-related proteins in infected plants. Annu. Rev. Phytopathol. **44:** 135–162.

Wang, L., and Brown, S.J. (2006). BindN: a web-based tool for efficient prediction of DNA and RNA binding sites in amino acid sequences. Nucleic Acids Res. **34:** W243–W248.

Wang, Y., Fan, X., Lin, F., He, G., Terzaghi, W., Zhu, D., and Deng, X.W. (2014). Arabidopsis noncoding RNA mediates control of photomorphogenesis by red light. Proc. Natl. Acad. Sci. USA **111:** 10359–10364.

Yu, D., Chen, C., and Chen, Z. (2001). Evidence for an important role of WRKY DNA binding proteins in the regulation of NPR1 gene expression. Plant Cell **13:** 1527–1540.

Zhang, X., Garreton, V., and Chua, N.H. (2005). The AIP2 E3 ligase acts as a novel negative regulator of ABA signaling by promoting ABI3 degradation. Genes Dev. **19:** 1532–1543.

Zhang, X., Henriques, R., Lin, S.S., Niu, Q.W., and Chua, N.H. (2006). Agrobacterium-mediated transformation of *Arabidopsis thaliana* using the floral dip method. Nat. Protoc. **1:** 641–646.

Zipfel, C., Kunze, G., Chinchilla, D., Caniard, A., Jones, J.D., Boller, T., and Felix, G. (2006). Perception of the bacterial PAMP EF-Tu by the receptor EFR restricts Agrobacterium-mediated transformation. Cell **125:** 749–760.